Applied Surface Science 257 (2010) 1161–1165

Contents lists available at ScienceDirect

Applied Surface Science

journal homepage: www.elsevier.com/locate/apsusc

Characterization of crystal lattice constant and dislocation density of crack-free GaN films grown on Si(1 1 1)

Jijun Xiong[a], Jianjun Tang[a], Ting Liang[a,b,*], Yong Wang[c], Chenyang Xue[b], Weili Shi[a], Wendong Zhang[a,b]

[a] North University of China, National Key Laboratory of Science and Technology on Electronic Test and Measurement Taiyuan 030051, PR China
[b] Key Laboratory of Instrumentation Science & Dynamic Measurement (North University of China), Ministry of Education Taiyuan 030051, PR China
[c] The 13th Research Institute, CETC, Shijiazhuang 050051, PR China

ARTICLE INFO

Article history:
Received 25 February 2010
Received in revised form 21 May 2010
Accepted 20 July 2010
Available online 21 August 2010

PACS:
87.85.Va
81.05.Ea
81.15.Gh
78.35.+c
61.05.C–

Keywords:
Metalorganic chemical vapor deposition
Semiconducting III–V materials
AFM
X-ray diffraction
Defects

ABSTRACT

GaN have sphalerite structure (Cubic-GaN) and wurtzite structure (hexagonal GaN). We report the H-GaN epilayer with a LT-AlN buffer layer has been grown on Si(1 1 1) substrate by metal-organic chemical vapor deposition (MOCVD). According to the FWHM values of 0.166° and 14.01 cm^{-1} of HDXRD curve and E_2 (high) phonon of Raman spectrum respectively, we found that the crystal quality is perfect. And based on the XRD spectrum, the crystal lattice constants of Si (a = 5.3354 Å) and H-GaN (a_{epi} = 3.214 Å, c_{epi} = 5.119 Å) have been calculated for researching the tetragonal distortion of the sample. These results indicate that the GaN epilayer is in tensile strain and Si substrate is in compressive strain which were good agreement with the analysis of Raman peaks shift. Comparing with typical values of screw-type (D_{screw} = 7 × 10^8 cm^{-2}) and edge-type (D_{edge} = 2.9 × 10^9 cm^{-2}) dislocation density, which is larger than that in GaN epilayers growth on SiC or sapphire substrates. But our finding is important for the understanding and application of nitride semiconductors.

© 2010 Published by Elsevier B.V.

www.spm.com.cn

1. Introduction

GaN is the most important semiconductor for the microelectronic and optoelectronic applications because of its excellent electrical properties such as wide band gap, high electron saturated velocity, high break down voltage, direct band gap and so on [1–3]. In another hand, GaN based MEMS hold many researchers' interesting due to its attractive mechanical properties [4,5]. GaN epitaxial films with quantum well structures are always growth on silicon carbide (SiC) or sapphire substrates and used in fabricating optoelectronic and microelectronic devices [6,7,8,9]. But in MEMS fields silicon substrates have much more importance than both kinds of substrates aforementioned. Sapphire is too stable to be micromachined and SiC is too expensive for large area application. On the contrary, Si micromachining technology is very mature and Si substrates are very cheap with respect to SiC substrates [10,11]. In spite of advantages of GaN/Si based MEMS, the crystal quality of GaN on Si substrates is lower than that on Sapphire and SiC substrates [12,13]. In the past few years the quality of GaN/Si is extremely increased due to the progresses of the buffer layer technologies and some important devices (HEMT, LEDs, etc.) are implemented by using GaN/Si [14,15]. In this work, crystal quality characteristics such as lattice constants, strain, residual stress and screw-type dislocation densities of GaN on Si(1 1 1) are systematically investigated by using HDXRD and temperature-dependent Raman spectroscopy. The results are useful in further of researching MEMS devices and integrated circuits (IC) based GaN/Si.

2. Experimental procedure

The GaN/LT-AlN/Si(1 1 1) samples were fabricated by the 13th Research Institute of CETC. N-type GaN epilayer was grown on Si(1 1 1) substrate by metal-organic chemical vapor deposition (MOCVD). The MOCVD system is Aixtron 200/4 HT-S. Trimethylgallium (TMGa), trimethylaluminum (TMAl), ammonia (NH_3) were used as Ga, Al and N sources respectively. H_2 was used as a carrier gas during AlN and GaN growth. The gas pressure in reactor was maintained at 2 × 10^4 Pa for both buffer and epitaxy layer pro-

* Corresponding author at: North University of China, National Key Laboratory of Science and Technology on Electronic Test and Measurement Taiyuan 030051, PR China. Tel.: +86 3513920330; fax: +86 3513922131.
E-mail address: liangting@nuc.edu.cn (T. Liang).

0169-4332/$ – see front matter © 2010 Published by Elsevier B.V.
doi:10.1016/j.apsusc.2010.07.073

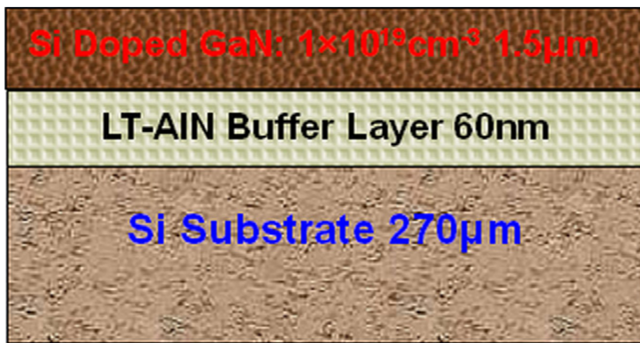

Fig. 1. Schematic view of GaN/Si(1 1 1) with the LT-AlN buffer system.

cesses. The schematic of epilayer structure is shown in Fig. 1 and the detailed growth processes is introduced as follow. Before loading the substrates, Si substrates were sequentially degreased by HCl: H_2O_2: H_2O (5:3:3) solutions for 5 min and etched in a HF: H_2O (1:10) solutions for 2 min, rinsed in deionized water and dried with pure N_2. At the beginning of the growth of AlN, the substrate was baked in an H_2 ambient at 1000 °C for 30 min to remove the native oxidation. Then AlN buffer layer was deposited at high-temperature (700 °C). After that, Si doped GaN film with dopant concentration of about 1×10^{19} cm^{-3} was grown at 1100 °C and annealing in N_2 ambient at 650 °C for 20 min. A nearly crack-free GaN epilayer of 1.5 μm-thickness with a 60 nm LT-AlN buffer layers grown on the Si(1 1 1) substrate was achieved [16]. Fig. 1 is schematic diagram of our sample.

The surface morphology of our samples were investigated by contact-mode atomic force microscopy (AFM, Model No 5500 of Benyuan GZ.). The grown samples were characterized by Raman spectroscopy (RENISHAW inVia) and X-ray diffraction (XRD) analysis. Raman spectra were measured using a 30 mW Ar^+ green light (514 nm) laser as an excitation source. The XRD was performed using a Bruker D-8AVANCE diffractometer system. The lattice constants of GaN and dislocation density in GaN epilayer were estimated according to the results of XRD measurements.

3. Results and discussion

3.1. Morphology observation

The surface morphology of the GaN layer grown on LT-AlN buffer layer is extremely smooth. Fig. 2(a) and (b) show the two-dimensional (2D) surface roughness and three-dimensional (3D) morphology characteristics images of GaN epitaxial films in a area of 2.0 μm × 2.0 μm. Using the software of CSPM Imager 4.60 for data processing and surface roughness analysis, We observed that the GaN/LT-AlN/Si (1 1 1) has a smooth surface, and the steps are not clear, which indicates that the quality of GaN epilayer is excellent. According to the surface roughness analysis of GaN epitaxial films, we can obtain that the surface roughness (Sa) reach 0.378 nm, the Root Mean Square (Sq) is 0.513 nm and the maximum peak-to-peak is 5.12 nm. These results demonstrated that it is possible to grow high-quality GaN films on Si by MOCVD. These values are comparable with other literature values for GaN on Si [17,18].

3.2. Raman testing

For H-GaN, two lines associated with A_1 (LO) and E_2 (high) optical phonon modes are expected in the first-order Raman spectra. Fig. 3 shows Raman spectra of the GaN/Si wafer. From the curve three peaks related to A_1 (LO), E_2 (high) modes of H-GaN and AO(TO)

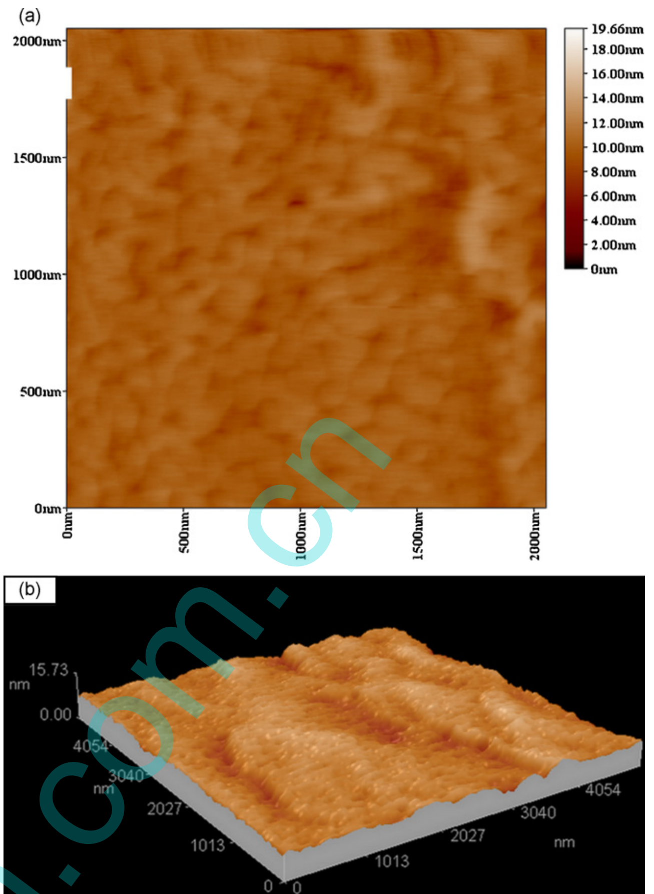

Fig. 2. 2D surface (a) and 3D morpholog feature (b) images by AFM in 2.0 μm × 2.0 μm

mode of Si substrate are clearly distinguished at 734.45, 566.94 and 521.22 cm^{-1}, respectively. The FWHM value of E_2 (high) mode is 14.01 cm^{-1}. Comparing with the Raman peaks of A_1 (LO) and E_2 (high) in bulk H-GaN located at 736 and 568 cm^{-1} [19], the red shifts of Raman peaks shown in Fig. 3 are observed. The reason should be ascribed to tensile stress in H-GaN epilayer. On the contrary, the Raman peak of Si(AO) has a blue shift which indicates compressive stress in the Si substrate. No Raman peaks of the cubic phase GaN can be seen in Fig. 3. It indicates that the GaN epilayer has high purity.

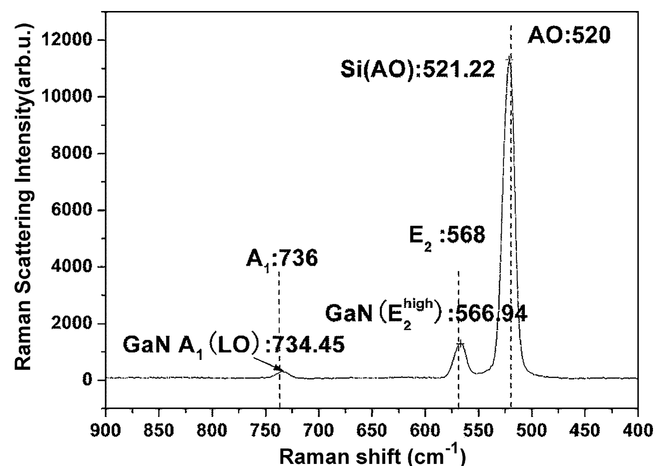

Fig. 3. Raman spectra of N-type GaN epilayer grown on Si substrate.

www.spm.com.cn

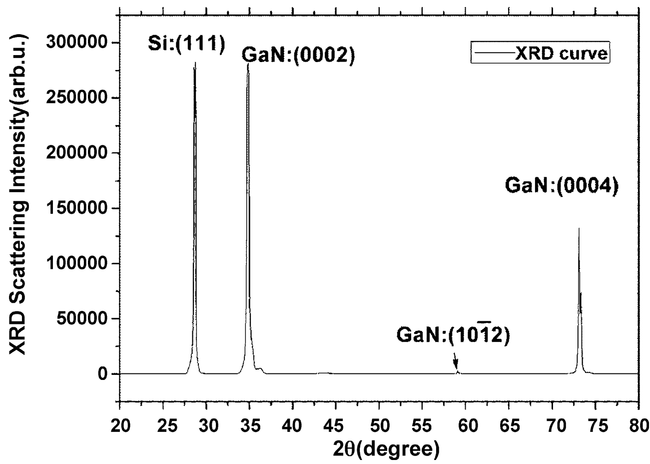

Fig. 4. X-ray diffrcation pattern of GaN epilayer.

3.3. Analysis of X-ray diffraction pattern

Fig. 4 shows the XRD curve of the GaN epilayer. It can be seen three clearly peaks related to H-GaN (0 0 0 2), (0 0 0 4) and Si (1 1 1). There is another faint peak related to H-GaN (10–12) at approx 56.8°.

The location of these peaks demonstrate that the GaN films are hexagonal wurtzite structure [20]. And no other peaks of cubic GaN appear in the spectra, indicating the single wurtzite GaN phase of the GaN epilayer. In the meanwhile the sharp diffraction peaks reveal that the single crystalline GaN epilayer have a high quality [21,22]. The symmetry analysis of the XRD revealed the GaN epitaxial mode growth with the hexagonal axis coinciding with the ⟨1 1 1⟩ direction of Si substrate.

3.4. Characterization of crystal lattice constants and strain

The lattice constants of the epitaxial GaN film were precisely determined by XRD symmetric and skew symmetric $\theta/2\theta$ scans in Fig. 4.

From the well known Bragg equation ($2d\sin\theta = n\lambda$), and reciprocal space can be calculated in Eq. (1) [23].

$$d_{hkl} = 1/\sqrt{\frac{4}{3}\left(\frac{h^2+hk+k^2}{a^2}\right)+\left(\frac{l^2}{c^2}\right)} \qquad (1)$$

We can calculate the lattice constants of H-GaN epilayer a_{epi} = 3.2022 Å and c_{epi} = 5.119 Å. Then the horizontal strain $\varepsilon_{//}$, vertical strain $\varepsilon_{\perp}$ and tetragonal distortion ε_T can be calculated by the expressions as follows: $\varepsilon_{//} = (a_{epi} - a_0)/a_0$, $\varepsilon_{\perp} = (c_{epi} - c_o)/c_o$, $\varepsilon_T = \varepsilon_{//} - \varepsilon_{\perp}$ [24], where a_0 and c_0 are the lattice constants of bulk H-GaN (a_0 = 3.189 Å, c_0 = 5.186 Å). The difference between c_{epi} and c_0 reveals that Si doped H-GaN epilayer on Si (1 1 1) substrate exhibits some in-plane tensile strain.

According to the results of biaxial strain values as $\varepsilon_{//}$ = 0.000413, $\varepsilon_{\perp}$ = −0.01292, $\varepsilon_T = \varepsilon_{//} - \varepsilon_{\perp}$ = 0.01705 in H-GaN epilayer, the Poisson ratio of about 0.32 of H-GaN epilayer can be derived which is approached to the theoretical value (ν_o = 0.305) [25].

The tetragonal distortion induced by tensile strain in GaN thin films is greater than zero, so it indicates that the tetragonal distortion is less than zero in Si substrate which caused by compressive stress consequentially. From the XRD results and Eq. (1) the lattice constants (a_{Si} = 5.3354 Å) of Si substrate can be calculated. It is smaller than relaxed C–Si (a_0 = 5.4309 Å). Existing of compressive stress in Si can be testified according to the difference between a_{Si} and a_0. So the GaN layer is found to be tensiley and compressively strained in the in-plane and out-of-plane directions, respectively, which is in agreement with the negative lattice mismatch between GaN and Si (1 1 1) [26].

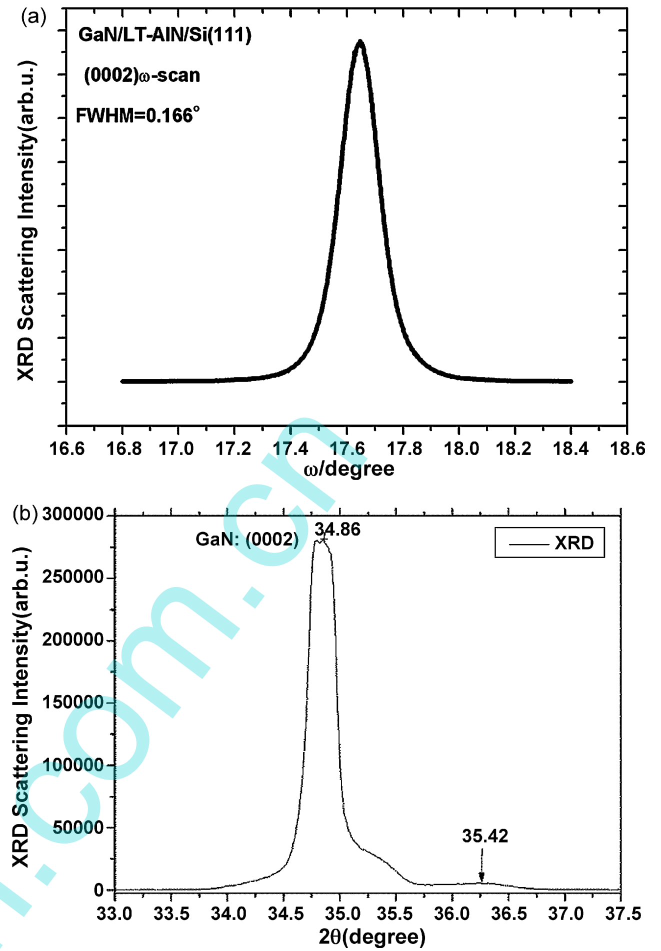

Fig. 5. (a) The X-ray rocking curve around the (0 0 0 2) reflection of GaN thin films growth on Si(1 1 1) by HDXRD and (b) 2θ curve of the sample, and the peak located at 34.86°.

Comparing with the tetragonal distortion of Si substrate ($\varepsilon_{T\text{-}Si}$ = −0.0176) and H-GaN epilayer ($\varepsilon_{T\text{-}GaN}$ = 0.01705) imply that the AlN buffer layer growth at low temperature exhibits good crystalline quality and low tensile stress in the layer. This finding suggests that the AlN buffer layer effectively reduce the biaxial strain localized at the interface of GaN epilayer and Si substrate [27].

3.5. Analysis of screw dislocation density

Owing to the lattice constants and thermal expansion coefficients differences between epilayer and substrate, dislocation and defects formed in the growth processes. To estimate the dislocation density in GaN epilayer, XRD was employed in θ–2θ scan mode and the curve is shown in Fig. 5. In Fig. 5(a), the sharp XRD diffraction peak of (0 0 0 2) reveals high crystalline quality in GaN epilayer. But a FWHM of 0.166° shows there is a slight deviation from perfect lattice. As showing in Fig. 5(b), the orientation of the mosaic structure related to the faint peak located at 35.42° distributed in a small range of 1.2° in the ⟨0 0 0 2⟩ direction. Fig. 6 shows rocking curves around the (10–12) reflection in the GaN films.

There are three main types of dislocations present in the GaN thin films: the pure edge dislocation with Burgers vector

www.spm.com.cn

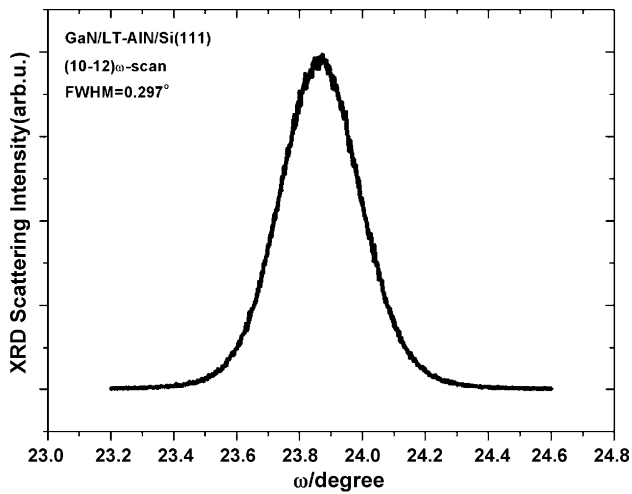

Fig. 6. The X-ray rocking curve around the (10–12) reflection by HDXRD

$b = 1/3\left\langle 11\ -20\right\rangle\ (a)$, the pure screw dislocation with Burgers vector $b = \langle 0\,0\,0\,1\rangle$ (c) and the mixed dislocation with $b = 1/3\left\langle 11 - 23\right\rangle\ (c + a)$.

$$D = \beta_{\mathrm{m}}^2(h\,k\,i\,l)/4.35b^2 \tag{2}$$

where β is the FWHM measured by XRD rocking curves and b is Burgers vector [24]. The value of the b_{c} can be calculated by the equation:

$$E_{\mathrm{screw}} = \mu b_{\mathrm{screw}}^2 = 2.65\,\mu a_{\mathrm{epi}}^2$$

$$E_{\mathrm{edge}} = \mu b_{\mathrm{edge}}^2/(1 - \nu) = 1.3\,\mu a_{\mathrm{epi}}^2 \tag{3}$$

where E_{screw} and E_{edge} are the strain energy of screw-type dislocation and edge-type dislocation, a_{epi} is the calculated lattice constant of GaN epilayer, ν is Poisson's ratio of H-GaN [28].

$$\beta_{\mathrm{m}}^2(h\ k\,i\,l) = \beta_0^2(h\,k\,i\,l) + \beta_{\mathrm{d}}^2(h\,k\,i\,l) + \beta_\alpha^2(h\,k\,i\,l) + \beta_{\mathrm{r}}^2(h\,k\,i\,l) + \beta_{\mathrm{l}}^2(h\,k\,i\,l) \tag{4}$$

where $\beta_{\mathrm{m}}{}^2(h\,k\,i\,l)$ is the FWHM value measured by rocking curve, $\beta_0{}^2(h\,k\,i\,l)$ is the intrinsic rocking curve, $\beta_{\mathrm{d}}{}^2(h\,k\,i\,l)$ is introduced by the apparatus, $\beta_\alpha{}^2(h\,k\,i\,l)$ is the rocking curve broadening caused by angular rotation in dislocation, $\beta_{\mathrm{r}}{}^2(h\,k\,i\,l)$ is the rocking curve broadening caused by the strain field, $\beta_{\mathrm{l}}{}^2(h\,k\,i\,l)$ is the rocking curve broadening due to the curvature of the film. Compared to $\beta_{\mathrm{m}}{}^2(h\,k\,i\,l)$ value, $\beta_0{}^2(h\,k\,i\,l)$, $\beta_{\mathrm{r}}{}^2(h\,k\,i\,l)$ and $\beta_{\mathrm{l}}{}^2(h\,k\,i\,l)$ are so small to be negligible ($\beta_0{}^2(h\,k\,i\,l) \ll \beta_{\mathrm{d}}{}^2(h\,k\,i\,l) \ll \beta_{\mathrm{r}}{}^2(h\,k\,i\,l) \ll \beta_{\mathrm{l}}{}^2(h\,k\,i\,l) \ll \beta_{\mathrm{m}}{}^2(h\,k\,i\,l)$). And the strain energy relaxed through the crack in the sample grown by MOCVD method mostly. (In the surface of the sample, the cracks were often observed and distributed regularly.), so

$$\beta_{\mathrm{m}}^2(h\ k\,i\,l) = \beta_\alpha^2(h\,k\,i\,l) \tag{5}$$

Combined Eq. (2), Eq. (3) and Eq. (5) the density is calculated of $D_{\mathrm{screw}} = 7 \times 10^8\ \mathrm{cm}^{-2}$ and $D_{\mathrm{edge}} = 2.9 \times 10^9\ \mathrm{cm}^{-2}$. The dislocation density D_{dis} of GaN films can be calculated from the equations: $D_{\mathrm{dis}} = D_{\mathrm{screw}} + D_{\mathrm{edge}} = 3.6 \times 10^9\ \mathrm{cm}^{-2}$.

Comparing with typical values of screw-type (10^6–$10^8\ \mathrm{cm}^{-2}$) and edge-type (10^7–$10^9\ \mathrm{cm}^{-2}$) dislocation density in the GaN grown on SiC or sapphire, the values of D_{screw} and D_{edge} in MOCVD-GaN on Si(1 1 1) demonstrate that the quality of GaN epilayer crystal is perfect.

4. Conclusions

In summary, the present Raman spectroscopic and X-ray diffraction characterizations have demonstrated that GaN films grown on Si(1 1 1) substrate are wurtzite structure with the [0 0 0 2] crystal orientation. And the low FWHM values of 14.01 cm^{-1} in E_2 (high) mode Raman spectrum and 0.166° of the [0 0 0 2] direction in X-ray rocking curve show high purity of H-GaN.

According to the calculating results of lattice constants, biaxial strain and tetragonal distortion of our sample, we concluded that (i) Si substrate suffered a compressive stress and GaN epilayer suffered a tensile stress; (ii) the LT-AlN buffer layer play a critical role relaxed the stress in GaN films from the analysis of strain in GaN and Si.

By calculating and analysing the screw-type dislocation density of GaN epilayer, we have demonstrated that the heteroepitaxial growth of GaN has good single crystal quality. Comparing with the screw-type dislocation (10^6–$10^8\ \mathrm{cm}^{-2}$) and edge-type dislocation(10^8–$10^{10}\ \mathrm{cm}^{-2}$) densities of GaN growth on SiC and sapphire, the densities of GaN/Si approach $D_{\mathrm{screw}} = 7 \times 10^8\ \mathrm{cm}^{-2}$ and $D_{\mathrm{edge}} = 2.9 \times 10^9\ \mathrm{cm}^{-2}$ which indicate that it is adapt to fabricate MEMS devices based GaN/Si or integrate GaN devices on IC [29].

Acknowledgements

This work was supported by the National Natural Science Foundation of China (Grant No. 60806022).

References

[1] A.M. Morales, C.M. Lieber, Science 279 (1998) 208–211.
[2] S.N. Yi, J.H. Na, K.H. Lee, A.F. Jarjour, R.A. Taylor, Y.S. Park, T.W. Kang, S. Kim, D.H. Ha, G. Andrew, D. Briggs, Appl. Phys. Lett. 90 (2007) 1901–1903.
[3] E. Jablonovich, G.D. Gody, IEEE Trans. Electron Dev. 29 (1982) 300–304.
[4] V. Cimalla, J. Pezoldt, O. Ambacher, J. Phys. D: Appl. Phys. 40 (2007) 6386–6434.
[5] G. Flik, H. Eisenschmid, C. Raudzix, F. Schatz, W. Schoenenborn, P.H. Trah, Mater. Res. Soc. Symp. Proc. 687 (2002), B1.1.
[6] .A. Reiher, J. Blasing, A. Dadgar, A. Diez, A. Krost, J. Cryst. Growth 248 (2003) 563–567.
[7] S. Nakamura, M. Senoh, S. Nagahama, N. Iwasa, T. Yamada, T. Matsushita, H. Kiyoku, Y. Sugimoto, T. Kozaki, H. Umemoto, M. Sano, K. Chocho, Appl. Phys. Lett. 72 (2007) 2014–2016.
[8] H. Yaguchi, J. Wu, B. Zhang, Y. Segawa, H. Nagasawa, K. Onabe, Y. Shiraki, J. Cryst. Growth 195 (1998) 323–327.
[9] H.F. Liu, H. Chen, Z.Q. Li, L. Wan, Q. Huang, J.M. Zhou, N. Yang, K. Tao, Y.J. Han, Y. Luo, J. Cryst. Growth 218 (2000) 191–196.
[10] Y. Wang, C.S. Xue, H.Z. Zhuang, Z.P. Wang, D.D. Zhang, Y.L. Huang, W.J. Liu, Appl. Surf. Sci. 255 (2009) 7719–7722.
[11] F. William, L. Nola, X. Tianming, M. Andrew, W. Shenjie, Y. Hongbo, S. Christopher, J. Muhammad, I.T. Ferguson, J. Cryst. Growth 218 (2000) 191–196.
[12] P. Burgaud, L. Constancias, G. Martel, C. Savina, D. Mesnager, Microelectron Reliab. 47 (2007) 1653–1657.
[13] E. Calleja, M.A. SancheGarcia, F.J. Sanchez, F. Calle, F.B. Naranjo, E. Munoz, S.I. Molina, A.M. Sanchez, F.J. Pacheco, R. Garcia, J. Cryst. Growth 201/202 (1999) 296–299.
[14] A. Dadgar, C. Hums, A. Diez, J. Blasing, A. Krost, J. Cryst. Growth 297 (2006) 279–282.
[15] E. Iliopoulos, A. Adikimenakis, E. Dimakis, K. Tsagaraki, G. Konstantinidis, A. Georgakilas, J. Cryst. Growth 278 (2005) 426–429.
[16] T. Liang, J.J. Tang, J.J. Xiong, Y. Wang, C.Y. Xue, X.J. Yang, W.D. Zhang, Vacuum 84 (2010) 1154–1158.
[17] E. Arslan, M.K. Ozturk, A. Teke, S. Ozcelik, E. Ozbay, J. Phys. D: Appl. Phys. 41 (2008) 155317–155319.
[18] S. Fu, J. Chen, H. Zhang, C. Guo, W. Li, W. Zhao, J. Cryst. Growth 311 (2009) 3325–3328.
[19] A. Munkholm, C. Thompson, C.M. Foster, J.A. Eastman, G.B. Stephenson, P. Fini, S.P. DenBaars, J.S. Speck, Appl. Phys. Lett. 72 (1998) 2972–2974.
[20] F. William, L. Nola, X. Tianming, M. Andrew, W. Shenjie, Y. Hongbo, S. Christopher, J. Muhammad, I.T. Ferguson, J. Cryst. Growth 311 (2009) 4306–4310.
[21] H. Heinke, V. Kirchner, S. Einfeldt, D. Hommel, Appl. Phys. Lett. 77 (2000) 2145–2147.
[22] S.Q. Zhou, A. Vantomme, B.S. Zhang, H. Yang, M.F. Wu, Appl. Phys. Lett. 86 (2005), 081912-1–081912-3.
[23] M. Jamil, J.R. Grandusky, V. Jindal, F.-S. Shahedipour, S. Guha, M. Arif, Appl. Phys. Lett. 87 (2005), 082103-1–082103-3.

www.spm.com.cn

[24] C. Kisielowski, J. Kruger, S. Ruvimov, T. Suski, J.W. Ager, E. Jones, Z. Liliental Weber, M. Rubin, E.R. Weber, Phys. Rev. B 54 (1996) 17745–17749.
[25] J. Blasing, A. Reiher, A. Dadgar, J. Blasing, A. Reiher, A. Dadgar, A. Diez, A. Krost, Appl. Phys. Lett. 81 (2002) 2722–2724.
[26] S.Q. Zhou, A. Vantomme, B.S. Zhang, H. Yang, M.F. Wu, Appl. Phys. Lett. 86 (2005) 081912–081914.
[27] Z.H. Wu, A.M. Fischer, F.A. Ponce, T. Yokogawa, S. Yoshida, R. Kato, Appl. Phys. Lett. 93 (2008), 011901-1–011901-3.
[28] K.S. Hong, T. Yao, J.B. Kim, Y.S. Yoon, I.T. Kim, Appl. Phys. Lett. 77 (2000) 82–84.
[29] K. Kim, C.B. Park, Thin Solid Films 330 (1998) 139–145.

www.spm.com.cn